Invited paper at the
"1976 European Symp.
on Few-Particle Problems
in Nuclear Physics"
Vlieland, Sept. 1976.

ISTITUTO NAZIONALE DI FISICA NUCLEARE
Laboratori Nazionali di Frascati

LNF-76/50(P)
11 Ottobre 1976

Torino-Dubna-Frascati Collaboration: ELASTIC AND INELASTIC SCATTERING OF $\pi^{\pm}$ MESONS ON ^{4}He AND ^{3}He.

Servizio Documentazione
dei Laboratori Nazionali di Frascati
Cas. Postale 13 - Frascati (Roma)

Laboratori Nazionali di Frascati
Servizio Documentazione

LNF-76/50(P)
11 Ottobre 1976

Torino-Dubna-Frascati Collaboration(x): ELASTIC AND INELASTIC SCATTERING OF $\pi^{\pm}$ MESONS ON ^{4}He AND ^{3}He(o).

The experimental data on the interaction of $\pi^{\pm}$ on ^{4}He and ^{3}He, obtained by the Torino - - Dubna - Frascati collaboration, are presented. The elastic scattering of $\pi^{\pm}$ on ^{4}He and ^{3}He has been studied at the Laboratory of Nuclear Problems of the JINR. The π^+ inelastic and the π^- backward elastic scattering on ^{4}He have been studied at the LEALE Laboratory of Frascati.

Among the nuclear structures which can be used in the study of pion interaction and absorption mechanism, the α-cluster model appears to be rather attractive. Recent experimental results on pion absorption and scattering by even-even nuclei seems to be satisfactorily explained in terms of the α-model. According to the above considerations, the great interest for a detailed study of the pion-α particle interaction is fully justified, especially as far as inelastic reactions (with and without charge exchange) and absorption are concerned.

The differential cross-section measurements of elastic scattering of $\pi^{\pm}$ on ^{3,4}He were performed using a high-pressure (4 atm) helium self-shunted streamer chamber surrounded by a scintillation counters hodoscope, covering the angular interval (25° - 165°). Fig. 1a shows the experimental set-up[1] and Fig. 1b a picture of a (π^+, ^{4}He) elastic scattering event. The pion beam parameters and the method for the events selection are described in refs. (2, 3). The central beam

---

(x) This work is the result of the collaboration of the Italian National Institute of Nuclear Physics and the Accademia Nazionale dei Lincei with the Joint Institute for Nuclear Research of Dubna.

This experimental study has been performed by:

F. Balestra, E. Bollini, L. Busso, R. Garfagnini, G. Piragino
Istituto di Fisica dell'Università di Torino, and INFN - Sezione di Torino.

M. Albu, T. Angelescu, I.V. Falomkin, M.M. Kulyukin, V.I. Lyashenko, R. Mach, A. Mihul, N.M. Kao, F. Nichitiu, G.B. Pontecorvo, M.G. Sapozhnikov, A. Seraru, Yu.A. Shcherbakov, T.M. Troshev, N.I. Trosheva
Joint Institute for Nuclear Research, Dubna (USSR).

R. Barbini, C. Guaraldo, A. Maggiora, R. Scrimaglio
Laboratori Nazionali di Frascati.

(o) Invited paper at the "1976 European Symposium on Few-Particle Problems in Nuclear Physics" Vlieland, September 13-15, 1976 - presented by G. Piragino.

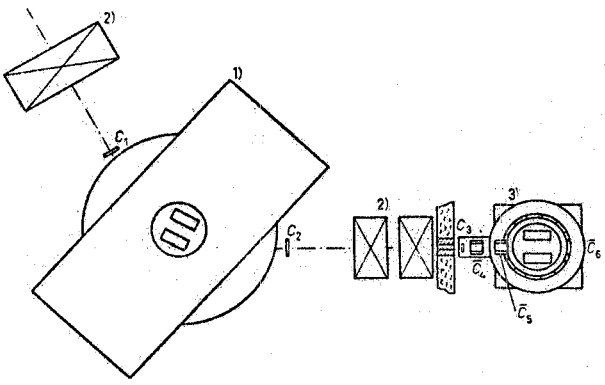

Fig. 1a - Diagram of the experimental set-up for ($\pi^{\pm}$, ^{4}He) and ($\pi^{\pm}$, ^{3}He) scattering measurements[1,2]:
1) bending magnet, with a helium streamer chamber at atmospheric pressure to measure the energy and the energy spread of the incoming $\pi^{\pm}$ beams; 2) quadrupole lenses; 3) helium filled streamer chamber (4 atm), surrounded by the hodoscope of scintillation counters (logic: C_1, C_2, C_3, C_4, C_5, C_6, C_{7-21}).

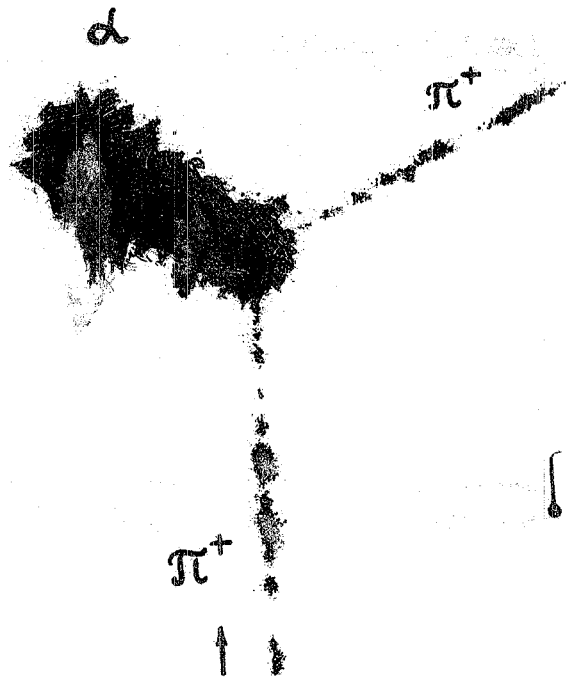

Fig. 1b - Typical (π^+, ^{4}He) elastic scattering event.

energy values were determined with a precision of (2 - 3) MeV and the energy spread was of (4-8)%, depending on the peak energy. The muon and electron beam contamination was measured with a total energy loss Cerenkov counter with a precision better than 3%. Fig. 2 shows the distribution of the parameters of the ($\pi^{\pm}$, ^{4}He) elastic scattering event of Fig. 1b, measured several times[3]. The deduced energy values of the incoming pions resulted in good agreement with the central energy of the beams. In the angular distributions, the events have been grouped in angular intervals, whose widths were chosen depending on the statistics we obtained. The cross-section measurements were performed for $\pi^{\pm}$, at 68, 98, 135, 145 and 156 MeV; for π^- also at 120, 174 and 208 MeV. Fig. 3 shows the experimental values for the ($\pi^{\pm}$, ^{4}He) differential cross-sections and the results of the optical model calculations with Laplacian and Mach potentials[4]. The results obtained using

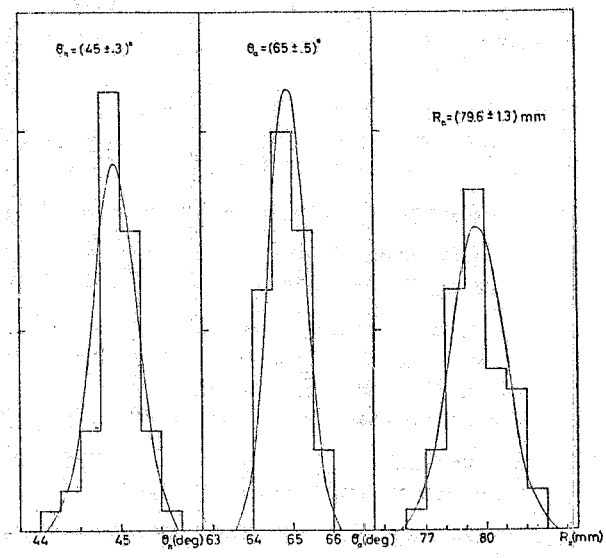

Fig. 2 - Distribution of the parameters of the event of Fig. 1b, measured several times.[3] All the data are reconstructed in the space ϑ_π: angle of the elastically scattered pion; ϑ_α: angle of the α-recoil; R_α: range of the α-recoil. From these data the energy of the incident pion turns out to be $E_\pi = (181 \pm 4)$ MeV and during that run the central pion-beam energy was (180 ± 9) MeV.

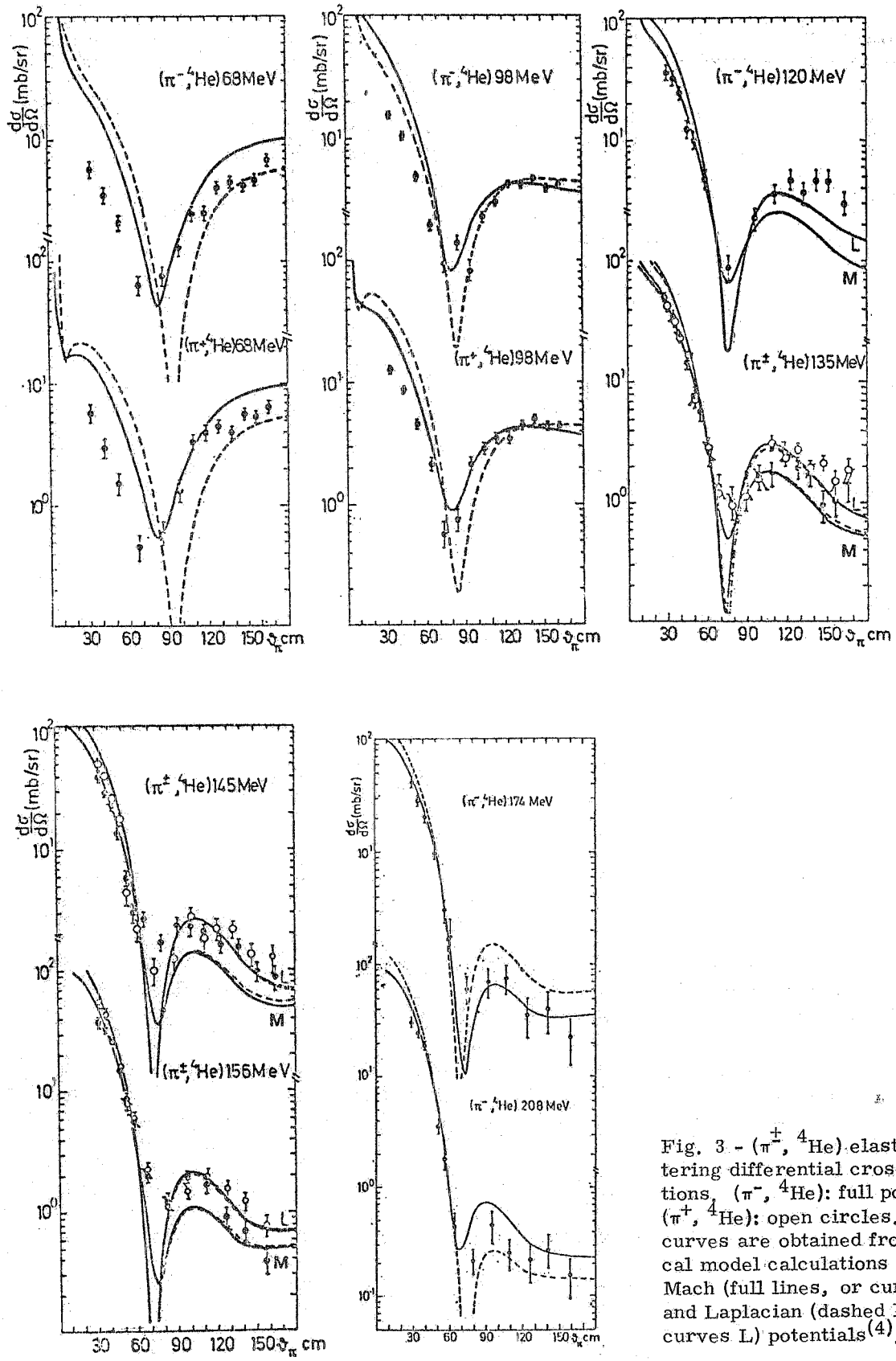

Fig. 3 - ($\pi^{\pm}$, ^{4}He) elastic scattering differential cross-sections, (π^-, ^{4}He): full points; (π^+, ^{4}He): open circles. The curves are obtained from optical model calculations using the Mach (full lines, or curves M) and Laplacian (dashed line, or curves L) potentials[4].

the Mach potential[5] are in better agreement with experimental data. Fig. 4 shows the comparison between our data and those obtained at 68 MeV by Crowe et al.[6] and at 180 MeV by Binon et al.[7];

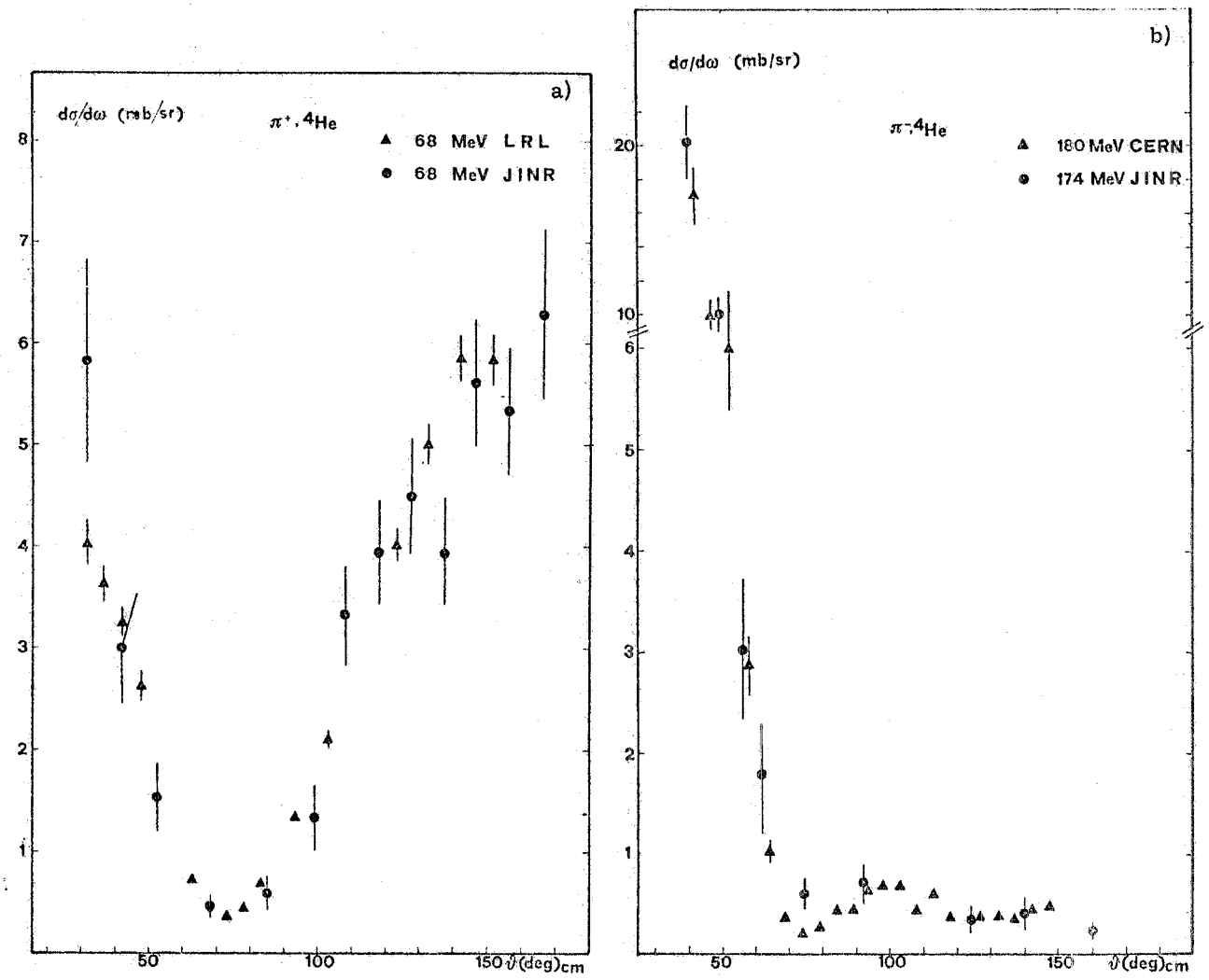

Fig. 4 - a) Comparison between (π^-, ^{4}He) elastic differential cross-section at E_π = 68 MeV and that obtained at the same energy by Crowe et al.[6]; b) Comparison between (π^-, ^{4}He) elastic differential cross-section at 174 MeV and that obtained at 180 MeV by Binon et al.[7].

the agreement is very good also for the differential cross-section at 174 MeV, where the angular behaviour has been obtained with rather poor statistics (about 400 events[4]). Fig. 5 shows the experimental values for the ($\pi^\pm$, ^{3}He) differential cross-sections and the results of the optical model calculations, using spin and isospin-dependent potentials[8]. There is rather good agreement between the experimental data and theoretical results; in general the statistics is not sufficient to discriminate between the Laplacian and the Mach potentials. An interesting feature observed in the ($\pi^\pm$, ^{4}He) and ($\pi^\pm$, ^{3}He) angular distributions is the fact that the minimum value of the cross sections occurs at about the same angles over the whole energy region ($\vartheta_\pi \simeq 75^\circ$ c.m.s.). The same effect was observed by Binon et al.[7] in (π^-, ^{4}He) elastic scattering measurements at (110 - 280) MeV, whereas for (π^-, ^{12}C) elastic scattering the angular position of the cross-section minimum shifts from 60° to 40° in the energy region (70 - 280) MeV[9]. The optical model calculations, using Mach potential describe qualitatively well the experimental data, the differential cross-section minima are correctly predicted, but there are discrepancies in the small angle region. These

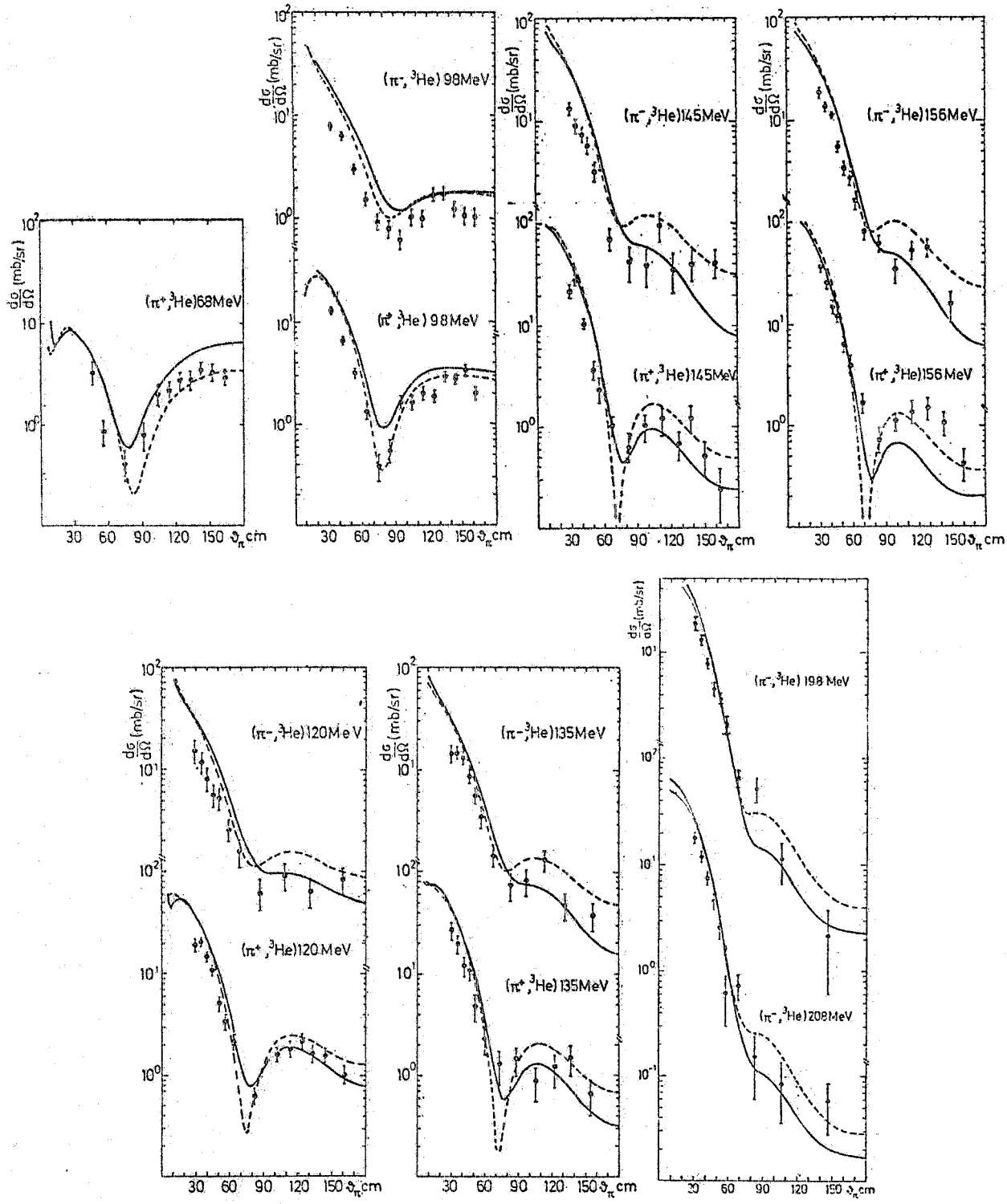

Fig. 5 - Differential cross-sections of ($\pi^{\pm}$, ^{3}He) elastic scattering. The curves represent the result of optical-model calculations with the Mach (full line) and Laplacian (dashed line) potentials[8].

differences between calculated and experimental results decrease with increasing pion energy. Fig. 6 shows the energy behaviour of the total cross-sections for ($\pi^{\pm}$, ^{4}He) and ($\pi^{\pm}$, ^{3}He) elastic scattering. Both energy behaviours of the experimental cross-sections show a resonance at about 150 MeV.

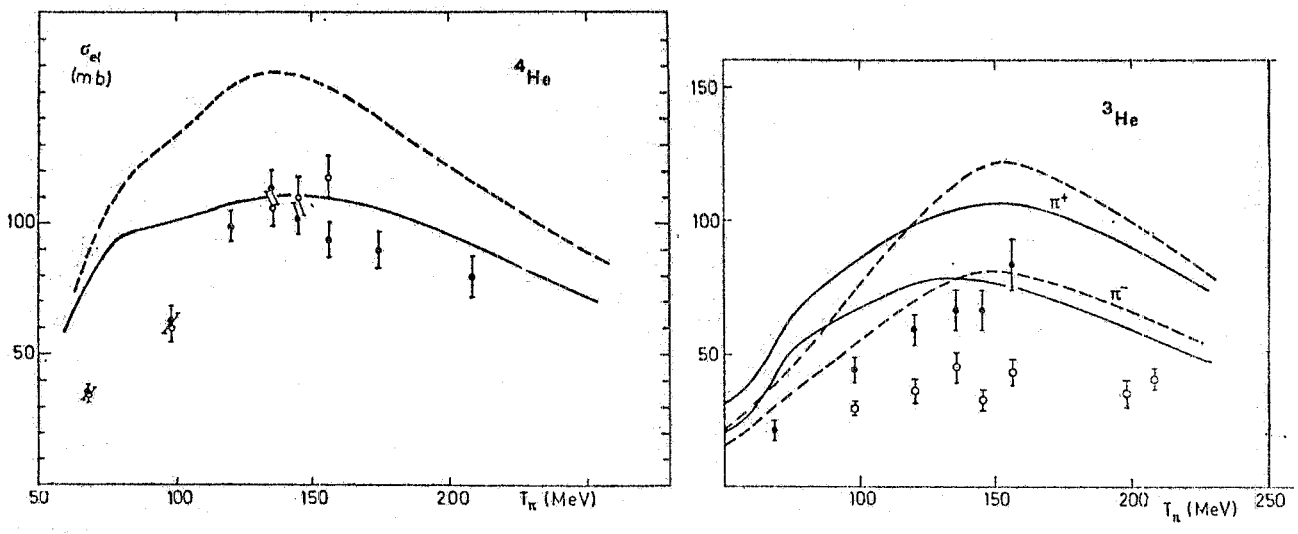

Fig. 6 - Energy behaviour of the total elastic cross-sections for ($\pi^{\pm}$, ^{4}He) and ($\pi^{\pm}$, ^{3}He) elastic scattering. The values were deduced by integrating from 0^o to 180^o the best-fit curves fitted by Legendre polynomials. The curves represent the optical model calculations with Mach (full line) and Laplacian (dashed line) potentials.

It must be noted that this behaviour is mostly determined by the forward part ($\vartheta < 75^o$) of the differential cross-section. The resonance position is reproduced by the optical model previsions, but there are evident quantitative discrepancies, in particular at energies lower than 100 MeV. Landau, at the Pittsburgh Conference[10] presented an improved optical potential for low and intermediate energies, which shows a very good agreement with our experimental data. Fig. 7 shows the comparison between our data and those obtained by Landau and Thomas[10] in the assumption that the pion-nucleon interaction can be described by a separable potential.

Figures 8 and 9 show the ($\pi^{\pm}$, ^{4}He) and ($\pi^{\pm}$, ^{3}He) elastic scattering differential cross-sections as a function of the squared momentum transfer $|t|$. As we can see, for $E_\pi > 100$ MeV, the con

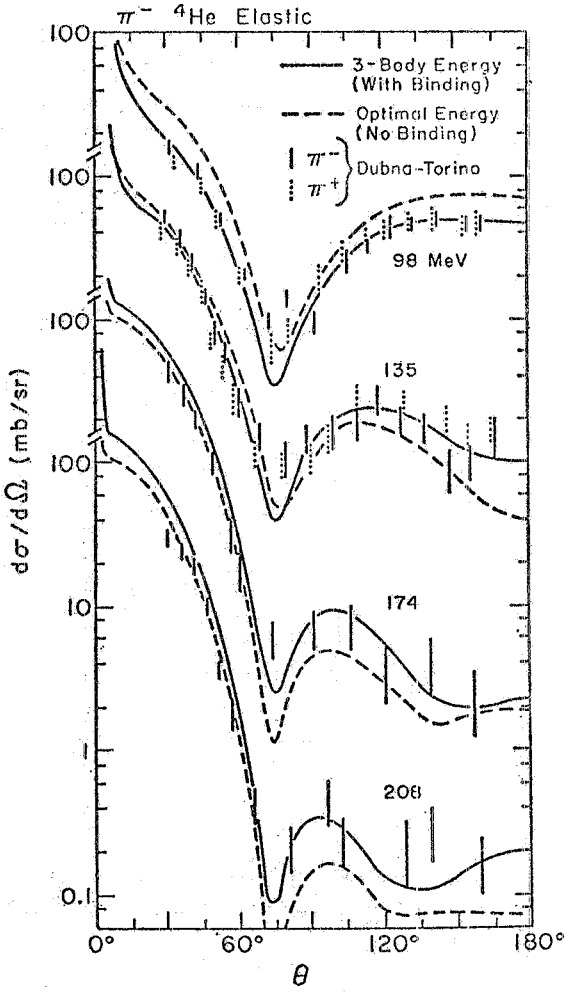

Fig. 7 - Comparison of (π^-, ^{4}He) differential cross-sections with the results, obtained by Landau and Thomas, using an improved optical model[10].

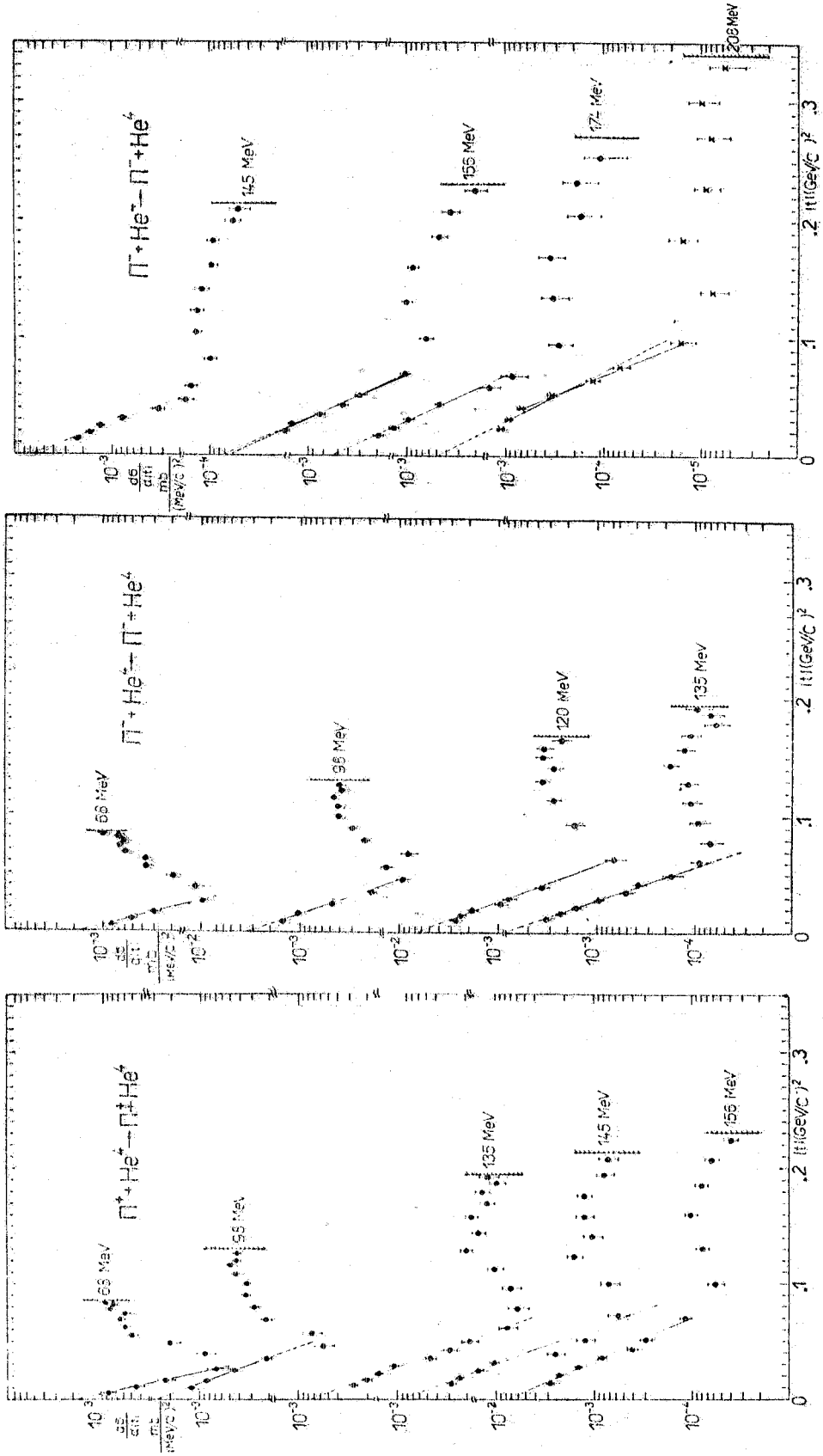

Fig. 8 - ($\pi^{\pm}$, ^{4}He) differential elastic cross-section as a function of the squared momentum transfer.

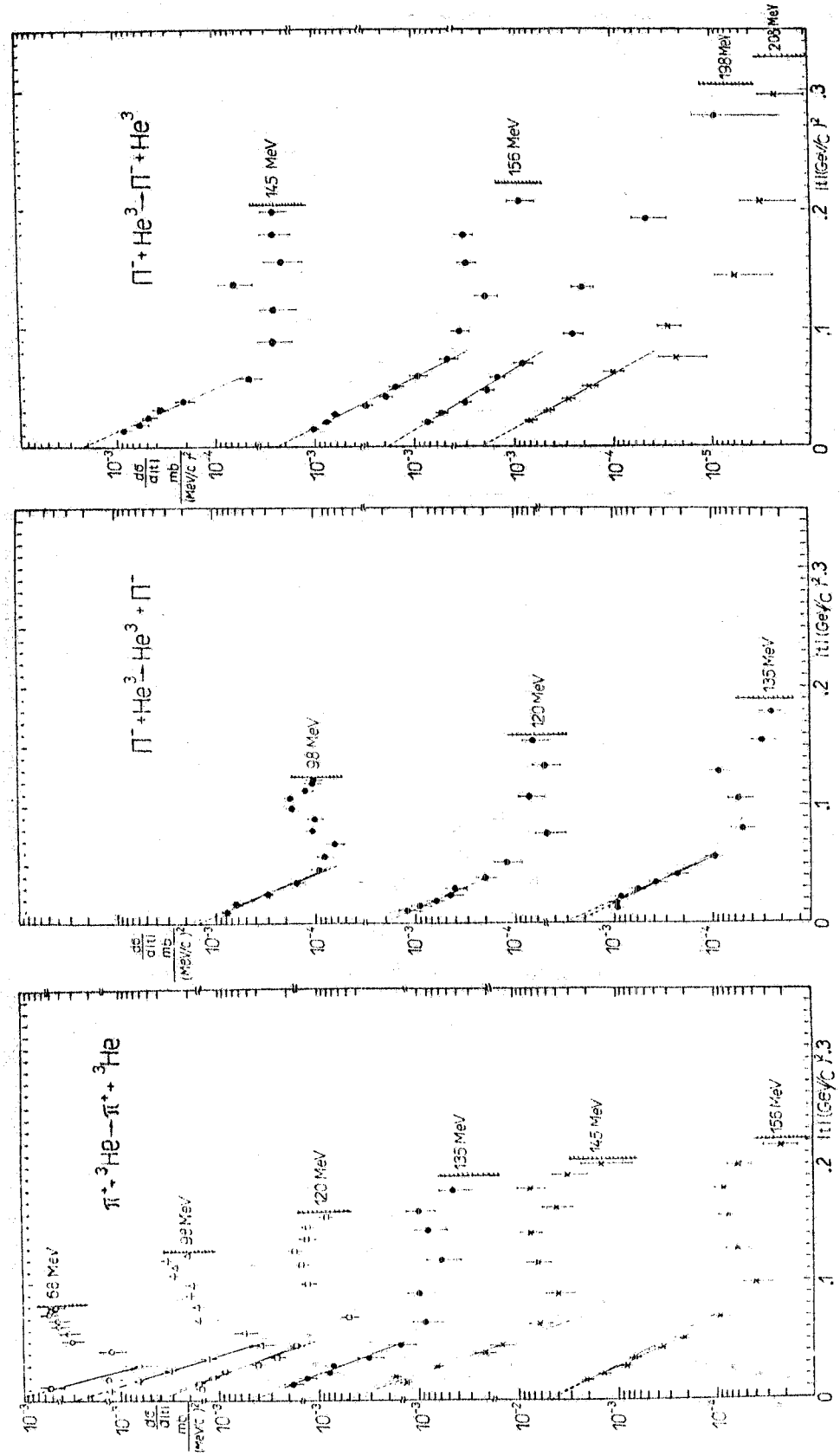

Fig. 9 - ($\pi^{\pm}$, ^{3}He) differential elastic cross-section as a function of the squared momentum transfer.

tribution of the non-exponential part of the cross-section respect to the total elastic cross-section, is negligible, and becomes more important and increases with the decreasing of the incoming pions energy. The larger values of the non-exponential part of the differential elastic cross-section occur at larger values of the squared momentum transfer, that is, in terms of angular distribution, in the region of backward scattered pions. Therefore, in agreement with Hüfner theoretical analysis[11], we can conclude that at low pion energies (E_π < 100 MeV) and at backward angles, the interaction cross-sections contain more informations on the nuclear structure.

Fig. 10 shows the large angle spectrometer we use at the Frascati Laboratory to measure the pion-nucleus backward scattering[12, 3]. With this experimental apparatus it is possible to measure the momentum ($\Delta p/p \sim$ $\sim 1\%$) of incoming and scattered pions by solid targets or by ^{4}He, which is the filling gas of the streamer chamber visualizing the pion tracks[3]. Fig. 11 shows the energy behaviour of the differential ($\pi^\pm$, ^{12}C) elastic scattering cross-section we measured at 175°. The maximum value of the differential cross-section is shifted to lower energy respect to the resonance energy of the total elastic cross-section[9]. The experimental data (ours and from refs. (9), (13)) are compared with the optical model previsions using Mach potential[5]. There is qualitatively agreement but at low energies the theoretical values are higher than the experimental

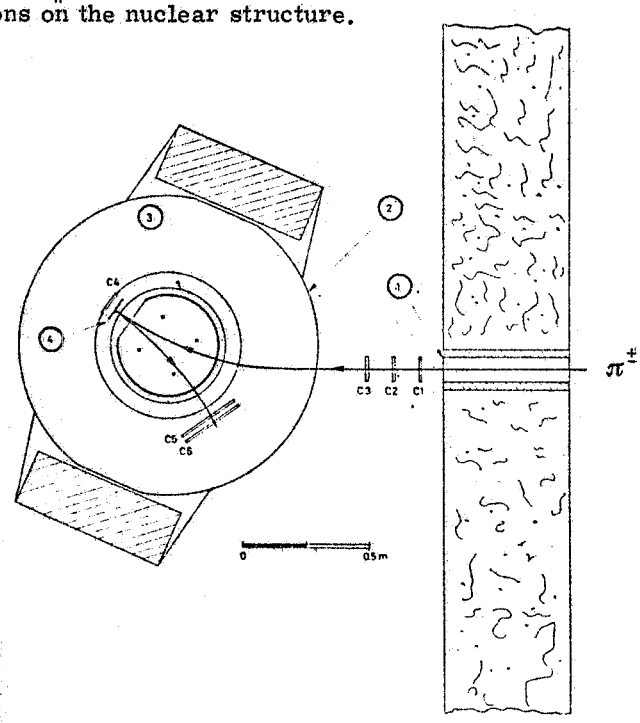

Fig. 10 - Layout of the experimental apparatus to measure the pion angular distribution at large angles. C_{1-6}: scintillation counters; (1) collimator 4 x 10 cm^2; (2) analyzing magnet; (3) helium self-shunted streamer chamber; (4) solid target $\sim 3 \times 40 \times 100$ mm^3. The trigger for hv-pulse generator is given by the logic : $(C_1, C_2, C_3, \bar{C}_4, C_5, C_6)$.

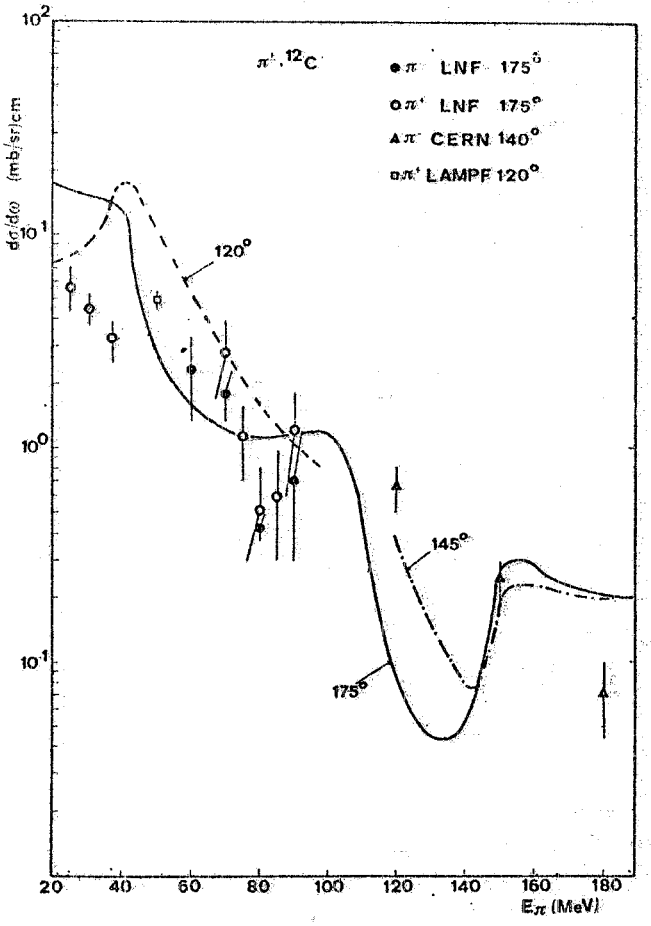

Fig. 11 - Energy behaviour of the backward ($\pi^\pm$, ^{12}C) elastic scattering differential cross-section. The theoretical curves have been calculated using the potential of Mach[5], for different angular values (ϑ = 120°, 145°, 175°) and for π^-. Full points: (π^-, ^{12}C) - present work; open circles: (π^+, ^{12}C) - present work, the low energy data are preliminary; square: ref. (13); triangles: ref. (9).

ones[14]. The same considerations can be done in the case of the large angle ($\pi^{\pm}$, ^{4}He) elastic scattering differential cross-section. Fig. 12 shows the value of the differential ($\pi^{\pm}$, ^{4}He) elastic scattering cross-section we obtained, compared with those from different experiments[6, 7, 15]. For

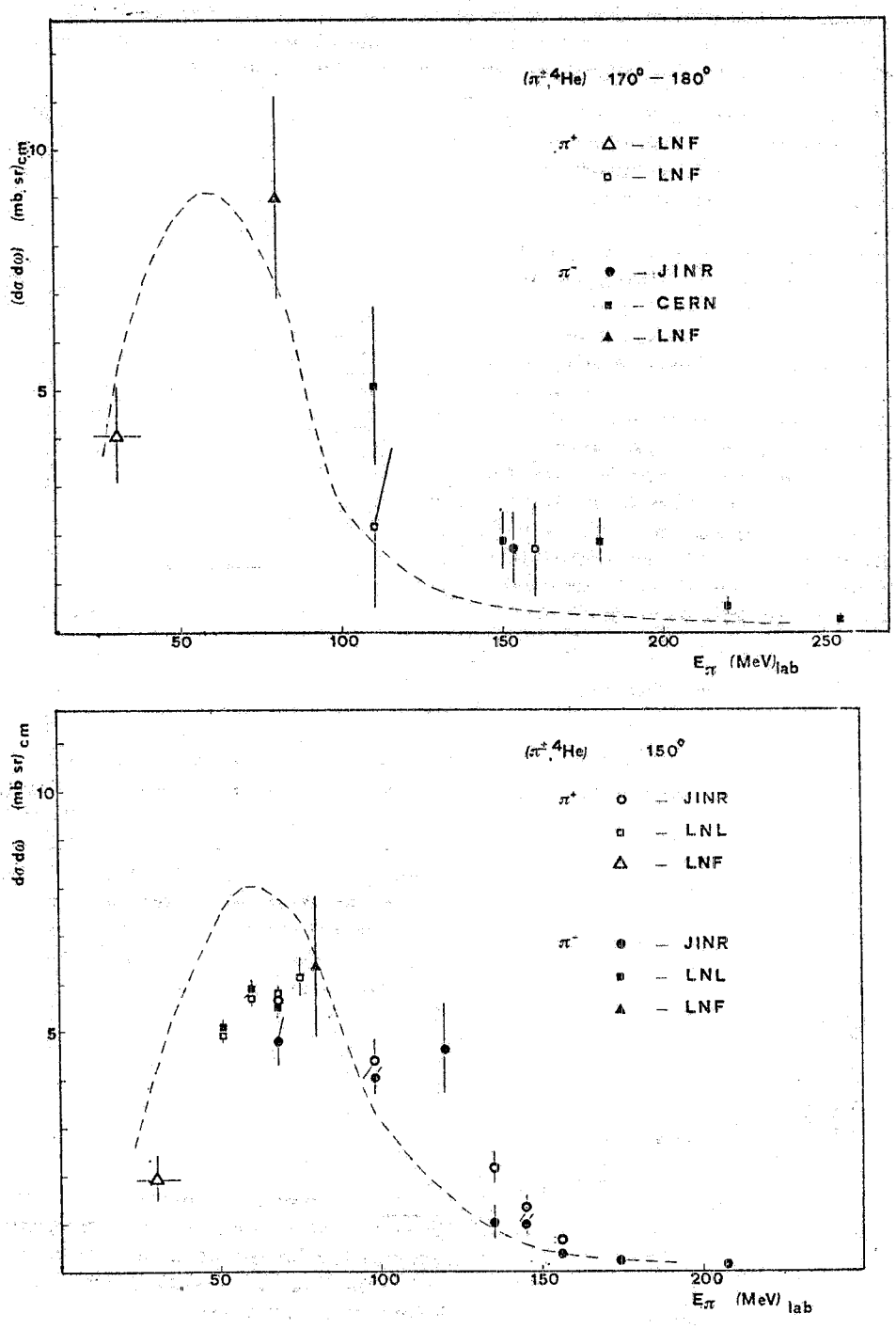

Fig. 12 - Energy behaviour of the backward ($\pi^{\pm}$, ^{4}He) elastic scattering differential cross-sections. The theoretical curves have been calculated using the potential of Mach, for π^-. The experimental data are from references : (4), (6), (7), (8), (15), (16) ; triangles : present work.

^{4}He again, the maximum value of the differential elastic cross-section takes place at low energy (at 40-70 MeV), comparing with the maximum of the total elastic cross section (at ~ 150 MeV) (Fig. 6). Fig. 13, deduced from ref. (17), shows the energy behaviour of the total and of the differential (at ~ 160°) elastic (π^-, p) scattering cross-sections. As we can see, the maximum is at about 180 MeV in both cases. Fig. 14 shows the energy bahaviour of the differential (π^+, d) ($\pi^\pm$, ^{3}He) elastic scattering cross-section at large angles (~160°). Here too, the shift to low energies of the resonance values, respect to the resonance value of total and backward differential (π^-, p) elastic cross sections, is more than 100 MeV.

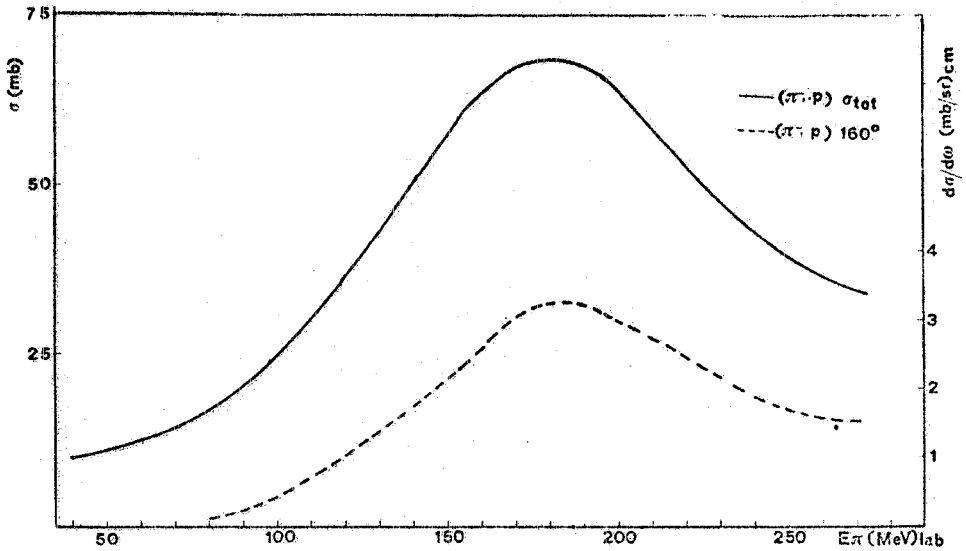

Fig. 13 - (π^-, p) total and differential (at ~ 160°) elastic scattering cross-section[17].

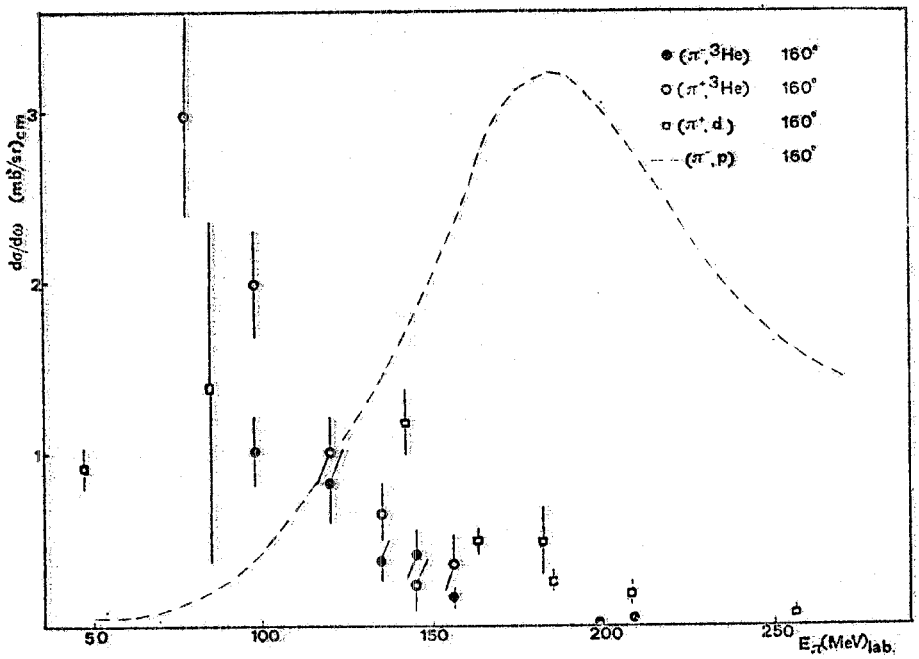

Fig. 14 - (π^+, d) and ($\pi^\pm$, ^{3}He) differential elastic scattering cross-sections (at about 160°), compared with the (π^-, p)$^{160°}$ elastic scattering cross-section (dashed line). The experimental ($\pi^\pm$, d)$^{160°}$ data are from ref. (18).

From this analysis of the differential pion elastic scattering data on d, ^{3}He, ^{4}He, ^{12}C, it turns out that, for angles lower than the first cross section minimum ($\sim 50^o$-70^o) and for energies higher than 100 MeV, the optical model, also in the black-disk model approximation, is in quite good agreement with experimental data. The energy behaviours of the differential cross-sections reproduce the energy behaviour of the total elastic cross-section. In the other angular region, in particular at large angles ($\vartheta > 150^o$), the energy behaviour of the differential cross-sections presents the resonance at low energy (about 100 MeV lower respect to the ($\pi^{\pm}$, p) differential elastic scattering cross section); furthermore, the optical model previsions, in particular for pion energies lower than 100 MeV, are not in good agreement with the experimental data. It seems possible to conclude that this effect, characterizing the pion-nucleus scattering, is connected to the nuclear structure contributions.

Of great interest are also inelastic and absorption processes. In Fig. 15 the cross-sections for the double charge exchange of π^+ on ^{4}He, we measured at JINR[19] with the experimental apparatus of Fig. 1a, are presented. The comparison with theoretical previsions[20, 21, 22] indicates that the model based on exchange current[21] gives a quite good description of the experimental results. However more definite conclusions can be drawn when new experimental data will be available.

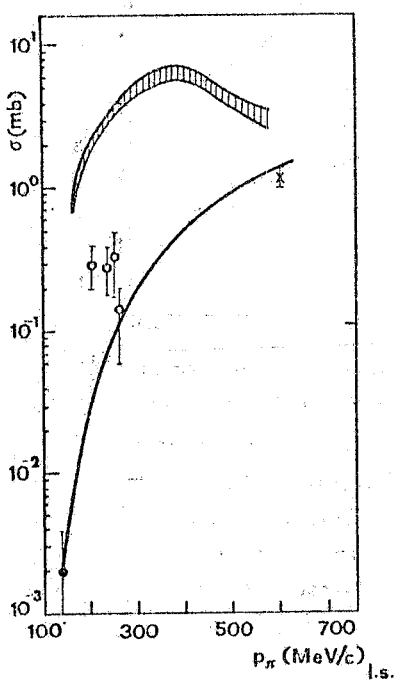

Fig. 15 - Cross-section of $\pi^+ + {}^4\text{He} \rightarrow \pi^- + 4p$ reaction as a function of the pion momentum. Upper curve: pair correlation prevision[20]; lower curve: exchange current model[21]; open circles: present work; cross: ref. (22); full point: from ref. (21).

Fig. 16 shows the apparatus we used to study the π^+ interaction on ^{4}He at the Frascati Laboratory[24]. The experiment has been carried out by using a diffusion cloud chamber, filled with helium at 15 atm, in magnetic field. The following reactions have been taken in consideration and analyzed:

$\pi^+ + {}^4\text{He} \rightarrow \pi^+ + {}^4\text{He}$			(1)
$\pi^+ + n + {}^3\text{He}$		(24%)	(1')
$\pi^+ + p + T$		(40%)	(2)
$\pi^+ + 2n + 2p$		(15%)	(3)
$\pi^+ + p + n + d$			
$\pi^o + p + {}^3\text{He}$		(15%)	(4)
$p + {}^3\text{He}$			
$\pi^o + n + 3p$		(6%)	(5)
$p + p + p + n$			
$p + p + d$			

In parenthesis are reported the percentages of occurence of each reaction normalized to the total number (793) of inelastic events. The experimental data have been grouped in two energy bins: (110 ± 12) and (160 ± 18) MeV. The elastic cross-sections[16] are in good agreement with the results we obtained at JINR[4]. The total cross-sections, corresponding to each reactions or groups of reactions, are reported in Table I[25].

We now analyse in detail reactions (2) and (1'). We will show that these reactions can be considered as resulting from a quasi-free scattering on individual bound nucleons, by assuming the residual nucleus not to partecipate directly to the interaction with the incoming pion. This point of view is supported by the experimental angular distributions of the nuclei. Moreover, the Fig. 17 shows the differential cross-sections of reaction (2) at 110 and 160 MeV, vs. the laboratory angle of the scattered pion, together with the cross-sections of the π^+ scattering from free protons ac-

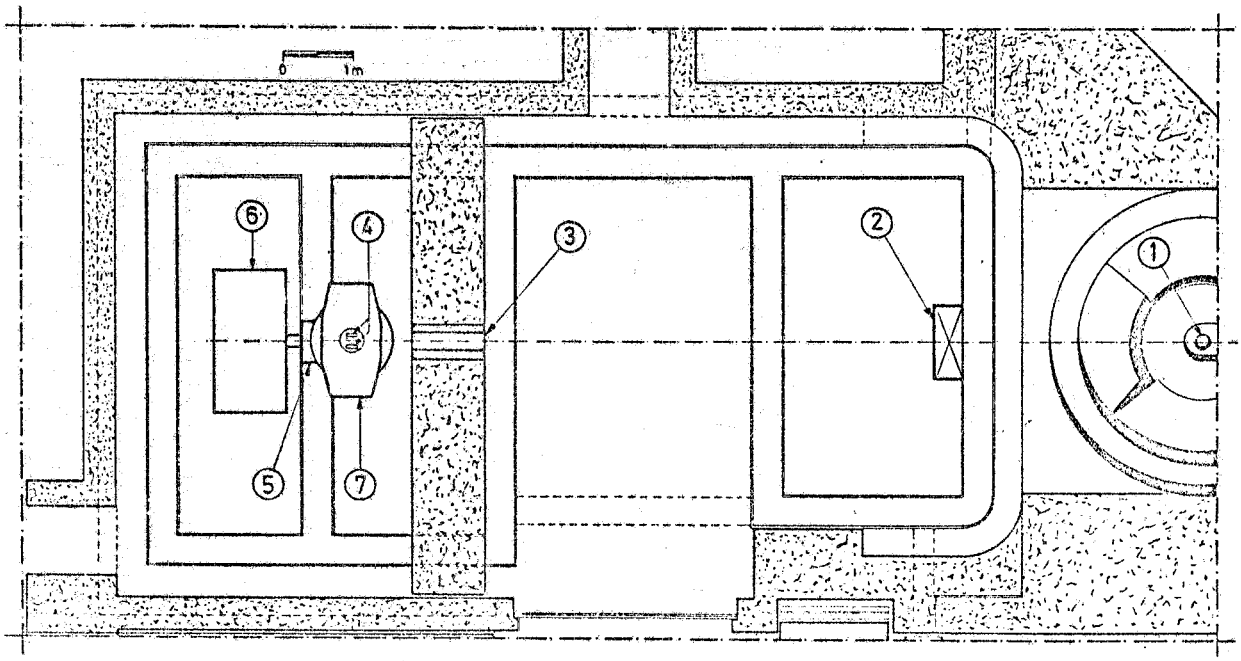

Fig. 16 - Layout of the experimental apparatus to study the (π^+, ^{4}He) interaction: 1) π^+ source; 2) quadrupole lens; 3) collimator (15 x 2) cm^2; 4) cameras; 5) flash unit; 6) refrigerator; 7) analyzing magnet and diffusion cloud-chamber.

TABLE I

		110 MeV	160 MeV
1	$\pi^+ + {}^4He \rightarrow \pi^+ + n + {}^3He$	$\sigma_T = (38.8 \pm 3.0)$ mb	$\sigma_T = (52.7 \pm 5.0)$ mb
2	$\pi^+ + {}^4He \rightarrow \pi^+ + p + t$	$\sigma_T = (84.6 \pm 7.3)$ mb	$\sigma_T = (102.3 \pm 7.6)$ mb
3	$\pi^+ + {}^4He \rightarrow \pi^+ + 2p + 2n$ $\pi^+ + p + n + d$	$\sigma_T = (39.0 \pm 4.9)$ mb	$\sigma_T = (32.8 \pm 4.3)$ mb
4	$\pi^+ + {}^4He \rightarrow \pi^o + p + {}^3He$ $p + {}^3He$	$\sigma_T = (22.3 \pm 3.7)$ mb	$\sigma_T = (48.6 \pm 5.3)$ mb
5	$\pi^+ + {}^4He \rightarrow \pi^o + 3p + n$ $3p + n$ $p + p + d$	$\sigma_T = (13.1 \pm 3.0)$ mb	$\sigma_T = (15.1 \pm 3.1)$ mb

(a) $\vartheta_\pi \geq 10^o$

cording to the data reported by Giacomelli et al.[17]. From a comparison among the angular distributions plotted in Fig. 17, a fundamental similarity turns out to exist between the behaviour of $\pi^+ + {}^4He \rightarrow \pi^+ + p + t$ reaction and that of pion scattering from free proton.

Fig. 18 shows the behaviour of the cross-section for reaction (2), vs. the laboratory scattering angles between the incident π^+ and the proton and between the incident π^+ and the tritium.

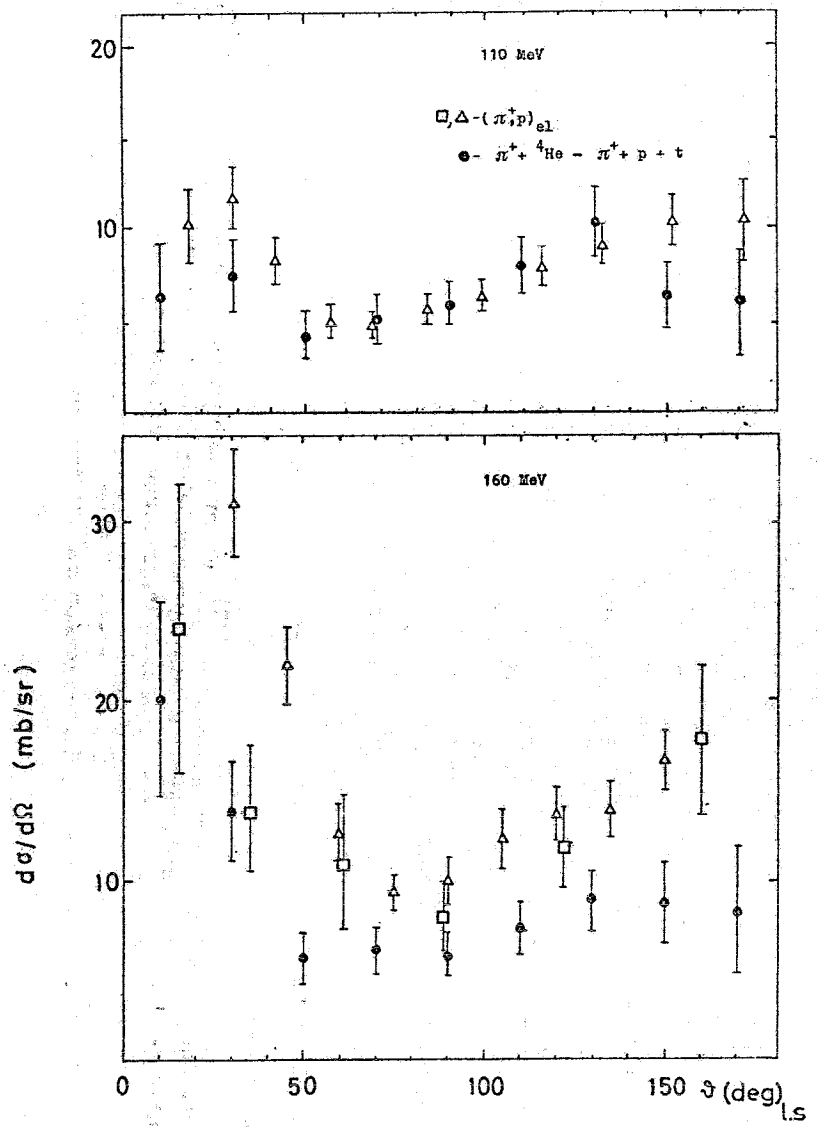

Fig. 17 - Differential cross-sections of the reaction $\pi^+ + {}^4He \rightarrow \pi^+ + p + t$, at 110 and 160 MeV, vs. the laboratory angle of the scattering pion (full points), compared with the differential elastic cross-section of π^+ on proton[17] at about the same energies (open triangles and squares).

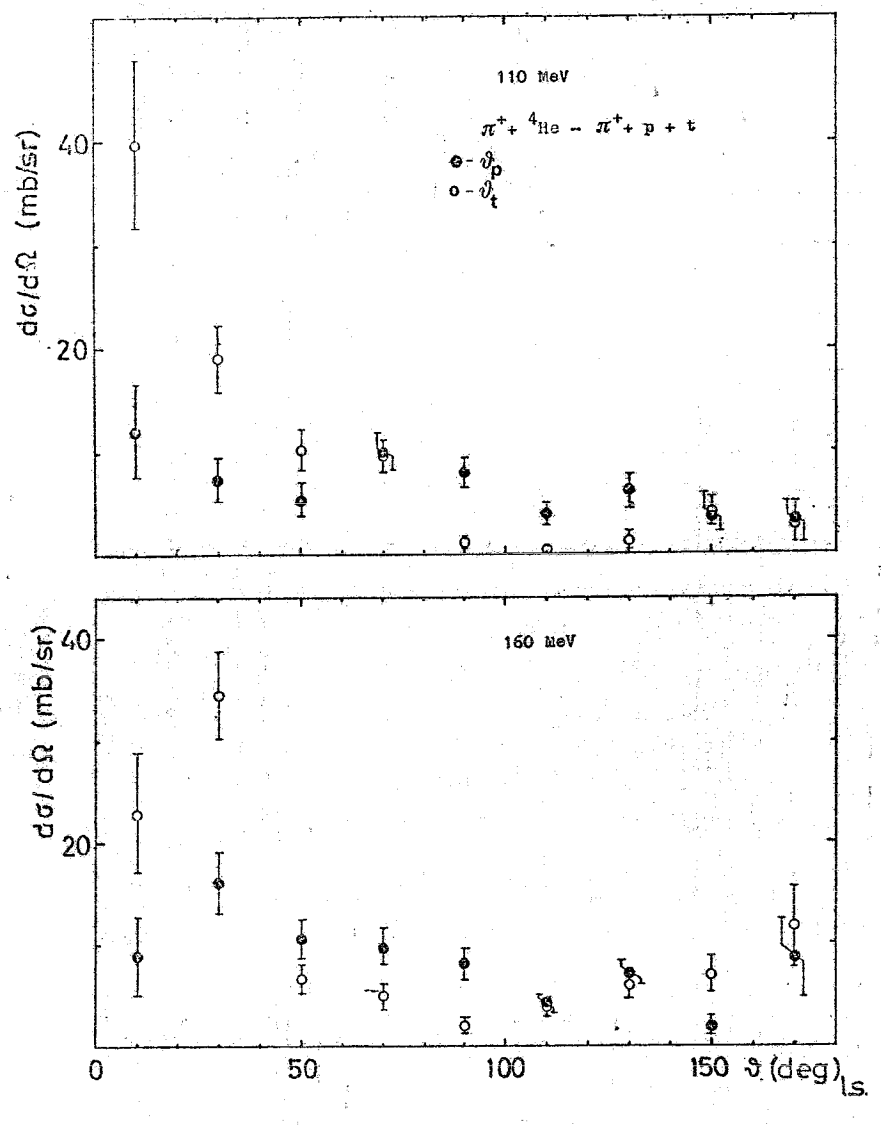

Fig. 18 - Differential cross-sections of the reaction $\pi^+ + {}^4He \rightarrow \pi^+ + p + t$, at 110 and 160 MeV, vs. the laboratory angle between the incoming π^+ and the proton (full points) and the triton (open circles).

for the two pion energies considered in this work. The analysis of the figures confirms our previous considerations upon the behaviour of the nuclei produced in reactions (1') and (2). More precisely, if such nuclei were involved as a whole in the interaction, some asimmetries should show up in the angular distributions of proton and tritium, corresponding to well defined kinematical correlations. On the contrary, the forward-backward asymmetry in the tritium distribution turns out to be fully consistent, within the experimental errors, with a quasi-spectator role played by this nucleus.

Fig. 19 shows the angular correlation between the proton and the scattered pion, both in reaction (2) and in scattering from free proton at the energies considered in this work. Here again the analogy is strictly in favour of a mechanism of direct interaction on a proton.

Fig. 20 shows for E_π = 110 and 160 MeV, the differential cross-sections of processes (1') and (2) vs. the laboratory angle of the scattered pion, together with the differences, at about the same energies of incoming pions, between the differential elastic cross-sections of the (π^+, ^{4}He) and the (π^+, ^{3}He) elastic scattering reactions of Figs. 3 and 5 respectively. From these differences one can infer the behaviour of the differential cross-section of π^+ scattering on bound neutron. Within the limits of the experimental errors, a good agreement is evident between the cross-section of process (1') and the differential elastic cross-sections. The differences between cross-sections of processes (1') and (2), which can in some way be ascribed to the different π-N isotopic spin states involved, give a further evidence for a direct interaction mechanism.

Figures 21a and 21b show the comparison[26] between our measurements at 160 MeV of the differential cross-section of the reactions $\pi^+ + {}^4\mathrm{He} \rightarrow \pi^+ + p + t$ and $\pi^+ + {}^4\mathrm{He} \rightarrow \pi^+ + n + {}^3\mathrm{He}$ and the differential cross-sections of the same reactions, induced by π^- at 153 MeV, obtained by Budagov et al.[15]. The value of the differential cross-section of the reaction π^+ on bound proton results higher than the differential cross-section of the reaction π^- on bound proton; in particular the ratio between the cross-sections, integrated in the (20°-180°) interval, results (8.4 ± 1.7). This value is very close to that, obtained[27] for free proton, of (9.8 ± 0.2). As a conclusion, we feel quite safe to state that the features of reaction (2), together with his relatively high probability of occurance, supports essentially a pion single nucleon interaction.

On the contrary, the ratio between integrated cross-section of the reactions, induced by $\pi^\pm$ on bound neutron, does not agree with the value obtained for the bound proton $(\sigma(\pi^-, n)_b/\sigma(\pi^+, n)_b = 1.3 \pm 0.2)$. It is interesting to note that the behaviour of the differential cross-sections $(\pi^+, p)_b$ and $(\pi^+, n)_b$, we obtained at 160 MeV for ^{4}He, are very similar to those, deduced for the deuterium by Norem[28] at 182 MeV. (Fig. 22).

We think to have shown that the low energy pion-nuclear physics is interesting and presents a lot of new important questions.

The authors would like to thank the Directorates of the Italian National Institute of Nuclear Physics, of the Accademia Nazionale dei Lincei and of the Joint Institute for Nuclear Research of Dubna, for their continuous encouragement and support during the experiments.

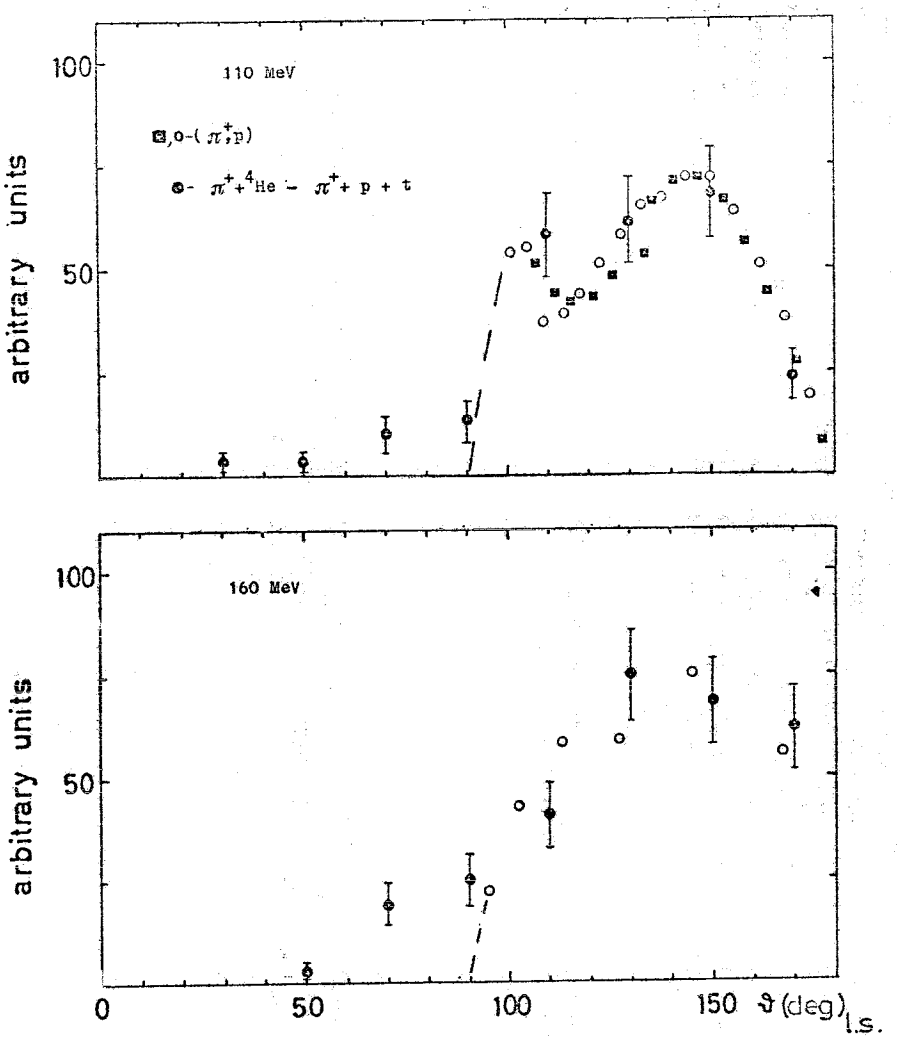

Fig. 19 - Differential cross-sections of the reaction $\pi^+ + {}^4He \rightarrow$ $\rightarrow \pi^+ + p + t$, at 110 and 160 MeV, vs. the laboratory angle between the scattered π^+ and proton, compared with the same angular distribution for (π^+, p) scattering[17]

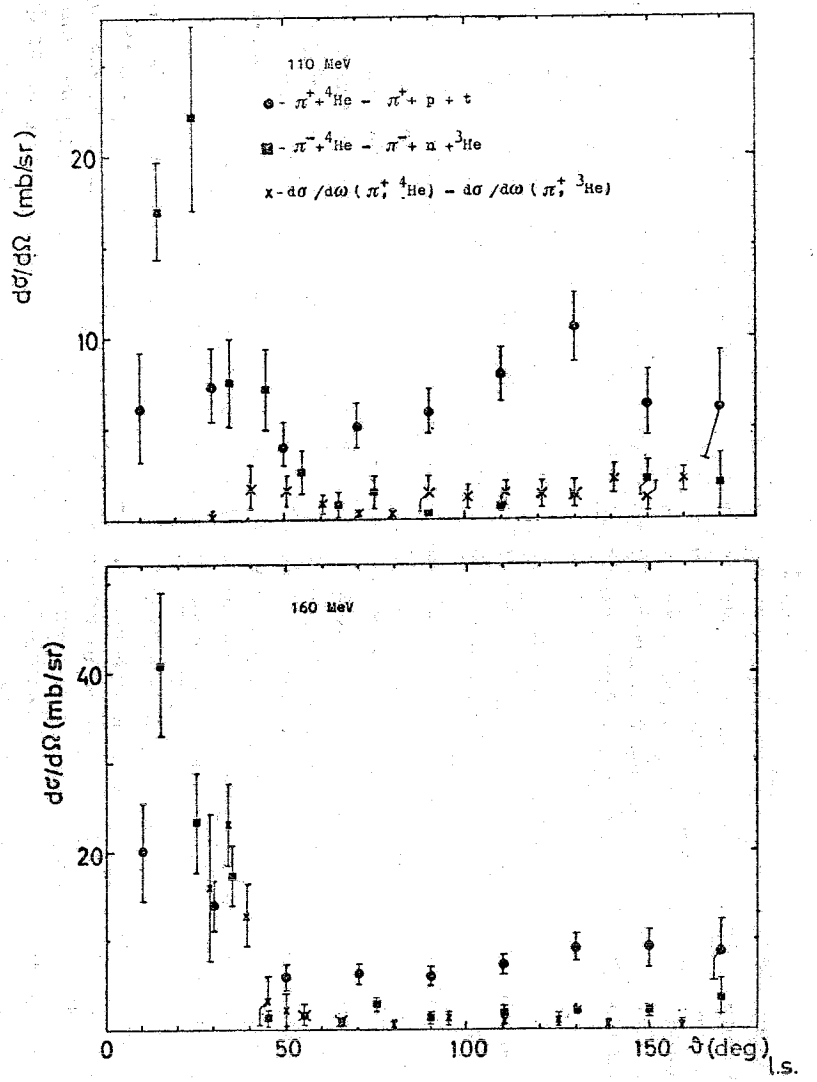

Fig. 20 - Differential cross sections of the reactions $\pi^+ + {}^4He \rightarrow$ $\rightarrow \pi^+ + p + t$ (points) and $\pi^+ + {}^4He \rightarrow \pi^+ + n + {}^3He$ (squares) and of the difference $\frac{d\sigma}{d\omega}(\pi^+, {}^4He)_{el} - \frac{d\sigma}{d\omega}(\pi^+, {}^3He)_{el}$ (crosses) at 110 and 160 MeV, vs. the laboratory angle of the scattered π^+

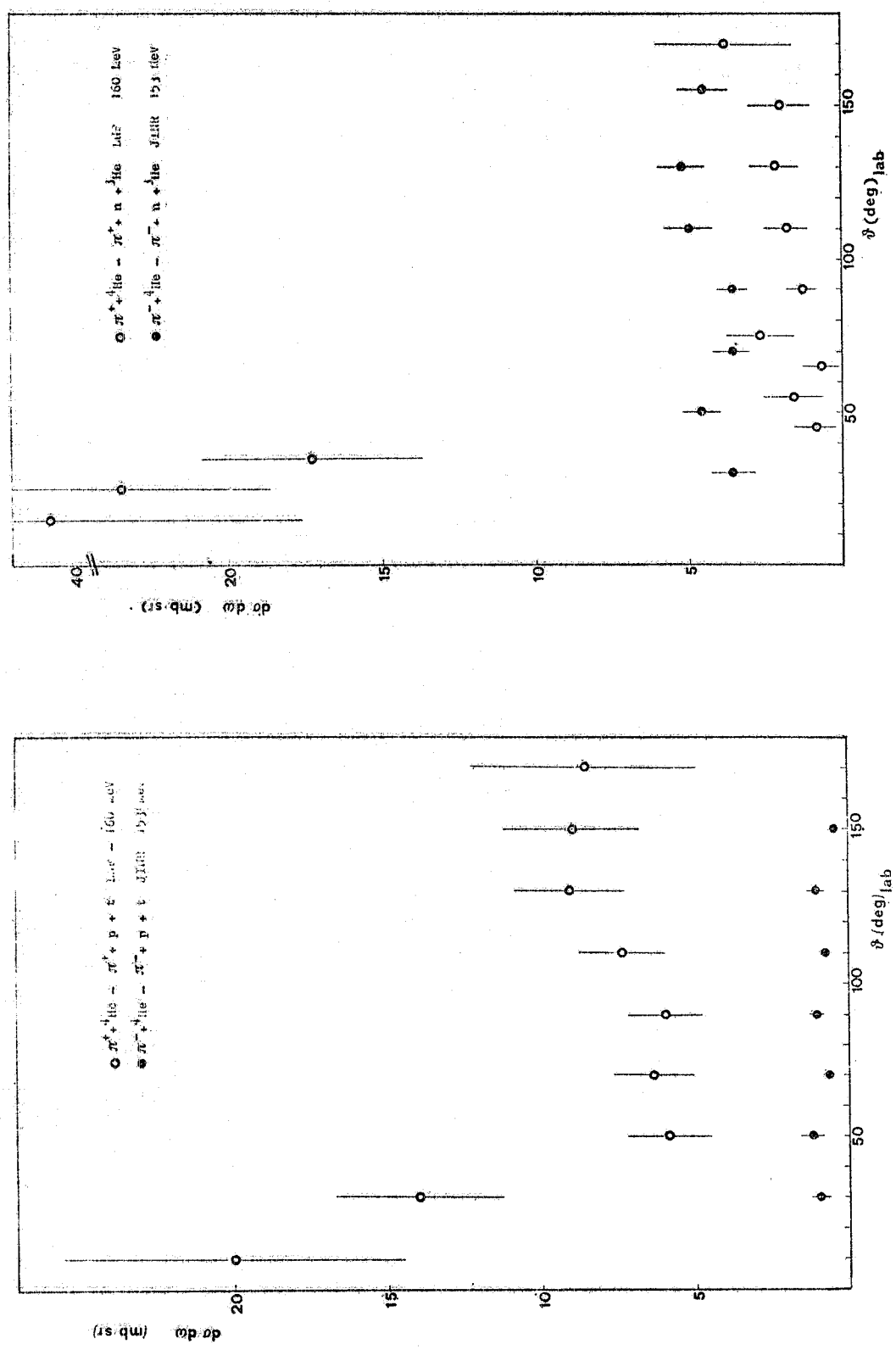

Fig. 21 - a) Differential cross-sections of the reactions $\pi^+ + {}^4He \rightarrow \pi^+ + p + t$ at 160 MeV (open circles) and $\pi^- + {}^4He \rightarrow \pi^- + p + t$ at 153 MeV(15) (full points); b) Differential cross-sections of the reactions $\pi^+ + {}^4He \rightarrow \pi^+ + n + {}^3He$ at 160 MeV (open circles) and $\pi^- + {}^4He \rightarrow \pi^- + n + {}^3He$ at 153 MeV(15) (full points).

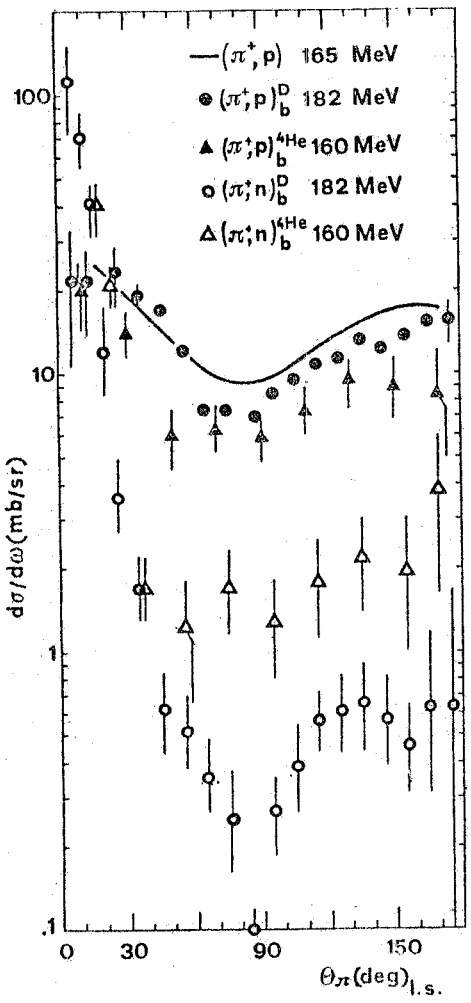

Fig. 22 - Differential cross section of π^+ scattering on bound proton and neutron. Full line: 165 MeV (π^+, p) elastic scattering[17]. Full points: 182 MeV $(\pi^+, p)_b$ in deuterium[28]. Open circles: 182 MeV $(\pi^+, n)_b$ in deuterium[28]. Triangles: 160 MeV $(\pi^+, p)_b$ and $(\pi^+, n)_b$ in ^{4}He (present work).

REFERENCES. -

(1) - I. V. Falomkin et al., Lett. Nuovo Cimento 3, 461 (1972); 5, 157 (1972).
(2) - M. Albu et al., Nuovo Cimento 21, 168 (1974).
(3) - F. Balestra et al., Nuclear Instr. and Meth. 125, 157 (1975).
(4) - Yu. A. Shcherbakov et al., Nuovo Cimento 31A, 249 (1976).
(5) - R. Mach, Nuclear Phys. A205, 56 (1973); Phys. Lett. 53B, 133 (1974).
(6) - K. M. Crowe et al., Phys. Rev. 180, 1349 (1969).
(7) - F. Binon et al., Phys. Rev. Letters 35, 145 (1975).
(8) - Yu. A. Shcherbakov et al., Nuovo Cimento 31A, 262 (1976).
(9) - F. Binon et al., Nuclear Phys. 17B, 168 (1970).
(10) - R. M. Landau and A. W. Thomas, Intern. Conf. on Meson-nucleon Physics, Pittsburgh (1976), pag. 30.
(11) - J. Hüfner, High Energy Physics and Nuclear Structure - 1975, AIP Conference Proceedings, n. 26.
(12) - F. Balestra et al., Nuclear Instr. and Meth. 119, 347 (1974).
(13) - J. F. Amann et al., Phys. Rev. Letters 35, 426 (1975).
(14) - C. Guaraldo et al., Lett. Nuovo Cimento 15, 368 (1976).
(15) - Yu. A. Budagov et al., Sov. Phys. -JETP 15, 824 (1962).
(16) - L. Busso et al., Few Particle Problems (North Holland Publ. Co., 1972), pag. 866.
(17) - G. Giacomelli et al., CERN-HERA 69-1 (1969).
(18) - D. Axen et al., Nuclear Phys. 256A, 387 (1976); K. C. Rogers et al., Phys. Rev. 105, 247 (1957); K. Gabathuler et al., Nuclear Phys. 55B, 397 (1973).
(19) - I. V. Falomkin et al., Lett. Nuovo Cimento 16, 525 (1976).
(20) - F. Becker and Yu. A. Batusov, Riv. Nuovo Cimento 1, 309 (1971).
(21) - J. F. Germond and C. Wilkin, Lett. Nuovo Cimento 13, 605 (1975).
(22) - A. T. Hess et al., Intern. Conf. on Meson-nucleon Physics, Pittsburgh (1976), pag. 106.
(23) - N. Carayannopulos et al., Phys. Rev. Letters 20, 1215 (1968).
(24) - R. Barbini et al., Nuclear Instr. and Meth. 102, 1 (1972).
(25) - F. Balestra et al., Lett. Nuovo Cimento 15, 535 (1976); 15, 542 (1976).
(26) - F. Balestra et al., Lett. Nuovo Cimento, in press.
(27) - P. J. Bussey et al., Nuclear Phys. 58B, 363 (1973).
(28) - J. H. Norem, Nuclear Phys. 33B, 512 (1971).